

# Pairing correlations in the two-leg Hubbard ladder

N. Bulut and S. Maekawa

*Institute for Materials Research, Tohoku University, Sendai 980-8577, Japan  
CREST, Japan Science and Technology Agency (JST), Kawaguchi, Saitama 332-0012, Japan*

(Dated: July 30, 2005)

In the ground state of the doped two-leg Hubbard ladder there are power-law decaying  $d_{x^2-y^2}$ -type pairing correlations. It is of interest to know the magnitude and the temperature scale of these correlations. For this purpose, determinantal Quantum Monte Carlo (QMC) simulations have been carried out for the reducible particle-particle interaction in the Hubbard ladder. Here, the results of these calculations are discussed. In particular, it is shown that, at sufficiently low temperatures, resonant particle-particle scattering takes place in the  $d_{x^2-y^2}$ -wave BCS channel for certain values of the model parameters. The QMC data presented here provide useful information about the strength of the  $d_{x^2-y^2}$  pairing correlations in the Hubbard ladder.

PACS numbers: 71.10.Fd, 71.10.Li, 74.20.Rp

The pairing correlations in the two-leg Hubbard model have been studied using various techniques of many-body physics. The Density Matrix Renormalization Group (DMRG) calculations found that the rung-rung pair-field correlation function decays as power law in the the ground state of the doped two-leg Hubbard ladder [1]. The mean-field calculations suggested the  $d_{x^2-y^2}$  type of symmetry for the pairing correlations in doped spin ladders [2]. The exact-diagonalization calculations found that the  $d_{x^2-y^2}$  type pairing correlations are enhanced when the interchain hopping  $t_{\perp}$  is greater than the intrachain hopping  $t$  [3]. The DMRG calculations found that the  $d_{x^2-y^2}$  type pairing correlations are strongest near half-filling for Coulomb repulsion in the intermediate coupling regime and  $t_{\perp} \approx 1.5t$  [4]. In this case, the Quantum Monte Carlo (QMC) calculations showed that the irreducible particle-particle interaction peaks for momentum transfers near  $(\pi, \pi)$  due to antiferromagnetic (AFM) fluctuations [5].

The two-leg Hubbard ladder is probably the only model where it is known from exact calculations that the pairing correlations get enhanced by turning on an onsite Coulomb repulsion in the ground state [3, 4]. Hence, it would be useful to know the characteristic temperature scale and the strength of the pairing correlations in this model. The QMC calculations of the particle-particle interaction which will be presented here have been carried out with this purpose.

In the following, the reducible particle-particle interaction  $\Gamma$  in the Bardeen-Cooper-Schrieffer (BCS) channel, illustrated in Fig. 1, will be studied for the two-leg Hubbard ladder by using QMC simulations. The reducible  $\Gamma$  is a useful probe of the pairing correlations. For example, in the case of an  $s$ -wave superconductor,  $\Gamma$  at the Fermi surface diverges to  $-\infty$ , when the superconducting transition is approached,  $T \rightarrow T_c^+$ , due to repeated particle-particle scatterings in the BCS channel. The QMC data which will be presented here show that, at sufficiently low temperatures,  $\Gamma$  for the doped Hub-

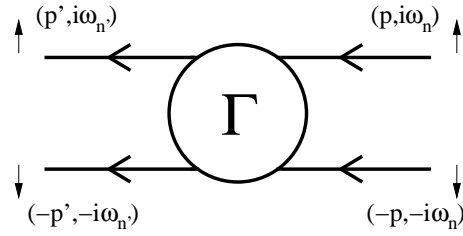


FIG. 1: Feynman diagram for the reducible particle-particle interaction  $\Gamma(p'|p)$  in the BCS channel.

bard ladder can become strongly repulsive (attractive) for scatterings near the Fermi surface with  $\mathbf{q} \approx (\pi, \pi)$  ( $\mathbf{q} \approx 0$ ) momentum transfers. This type of momentum dependence of  $\Gamma$  means that resonant scattering in the  $d_{x^2-y^2}$ -wave BCS channel is taking place at these temperatures. In order to determine the strength of the pairing correlations, the solution of the Bethe-Salpeter equation will be presented. These QMC results provide useful information about the maximum possible strength of the  $d_{x^2-y^2}$  pairing correlations in the Hubbard ladder.

The two-leg Hubbard model is defined by

$$H = -t \sum_{i,\lambda,\sigma} (c_{i,\lambda,\sigma}^\dagger c_{i+1,\lambda,\sigma} + \text{h.c.}) - t_{\perp} \sum_{i,\sigma} (c_{i,1,\sigma}^\dagger c_{i,2,\sigma} + \text{h.c.}) + U \sum_{i,\lambda} n_{i,\lambda,\uparrow} n_{i,\lambda,\downarrow} - \mu \sum_{i,\lambda,\sigma} n_{i,\lambda,\sigma}, \quad (1)$$

where  $t$  is the hopping parameter parallel to the chains (along  $\hat{\mathbf{x}}$ ), and  $t_{\perp}$  is for hopping perpendicular to the chains (along  $\hat{\mathbf{y}}$ ). The operator  $c_{i,\lambda,\sigma}^\dagger$  ( $c_{i,\lambda,\sigma}$ ) creates (annihilates) an electron of spin  $\sigma$  at site  $i$  of chain  $\lambda$ , and  $n_{i,\lambda,\sigma} = c_{i,\lambda,\sigma}^\dagger c_{i,\lambda,\sigma}$  is the electron occupation number. Here,  $U$  is the onsite Coulomb repulsion, and  $\mu$  is the chemical potential. In addition, periodic boundary conditions were used along the chains, and  $t_{\perp}$  denotes inter-chain hopping for open boundary conditions.

In obtaining the data presented here, the determinantal QMC technique described in Ref. [6] was used. The

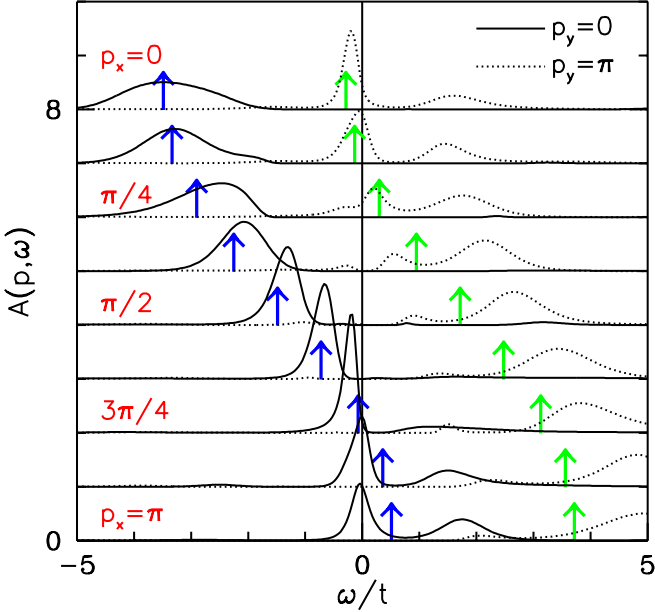


FIG. 2: (color online) Single-particle spectral weight  $A(\mathbf{p}, \omega)$  versus  $\omega$  at various  $\mathbf{p}$ . The solid and dotted curves represent the bonding ( $p_y = 0$ ) and antibonding ( $p_y = \pi$ ) bands, respectively. These results are for  $T = 0.1t$ ,  $U = 4t$ ,  $t_{\perp} = 1.6t$  and  $\langle n \rangle = 0.94$ . The arrows denote the quasiparticle positions for the  $U = 0$  case.

calculation of the reducible interaction  $\Gamma$  follows the procedure described in Ref. [7] for the two-dimensional (2D) case. The BCS component of the reducible particle-particle interaction  $\Gamma(p'|p)$  is illustrated in Fig. 1, where  $p = (\mathbf{p}, i\omega_n)$  with Matsubara frequency  $\omega_n = (2n+1)\pi T$ . Here the incoming fermions at states  $(\mathbf{p}, i\omega_n)$  with up spin and  $(-\mathbf{p}, -i\omega_n)$  with down spin scatter to states  $(\mathbf{p}', i\omega_{n'})$  with up spin and  $(-\mathbf{p}', -i\omega_{n'})$  with down spin by exchanging momentum  $\mathbf{q} = \mathbf{p}' - \mathbf{p}$  and Matsubara frequency  $\omega_m = \omega_{n'} - \omega_n$ . In the following, results will be shown for the reducible interaction in the singlet channel,  $\Gamma_s(p'|p) = \frac{1}{2}[\Gamma(p'|p) + \Gamma(-p'|p)]$ . In particular, the momentum dependence of  $\Gamma_s(\mathbf{p}', i\omega_{n'} | \mathbf{p}, i\omega_n)$  will be shown at the lowest Matsubara frequency  $\omega_n = \omega_{n'} = \pi T$ . In the ground state and for  $U = 4t$ , the  $d_{x^2-y^2}$  type of pairing correlations are most enhanced near half-filling for  $t_{\perp} \approx 1.6t$  [4]. When  $U = 8t$ , this occurs for  $t_{\perp} \approx 1.4t$ . In this paper, the QMC data will be presented using these parameter sets for a  $2 \times 16$  lattice.

The momentum structure in  $\Gamma_s(p'|p)$  depends sensitively on where  $\mathbf{p}'$  and  $\mathbf{p}$  are located with respect to the Fermi surface. Hence, first results on the single-particle spectral weight  $A(\mathbf{p}, \omega)$  will be shown, and the location of the Fermi-surface crossing points will be discussed. The results on  $A(\mathbf{p}, \omega)$  were obtained from the QMC data on the single-particle Green's function with the maximum-entropy method. Figure 2 shows  $A(\mathbf{p}, \omega)$  versus  $\omega$  for the parameters  $T = 0.1t$ ,  $U = 4t$ ,  $t_{\perp} = 1.6t$  and  $\langle n \rangle = 0.94$ . Here, it is seen that the Fermi level

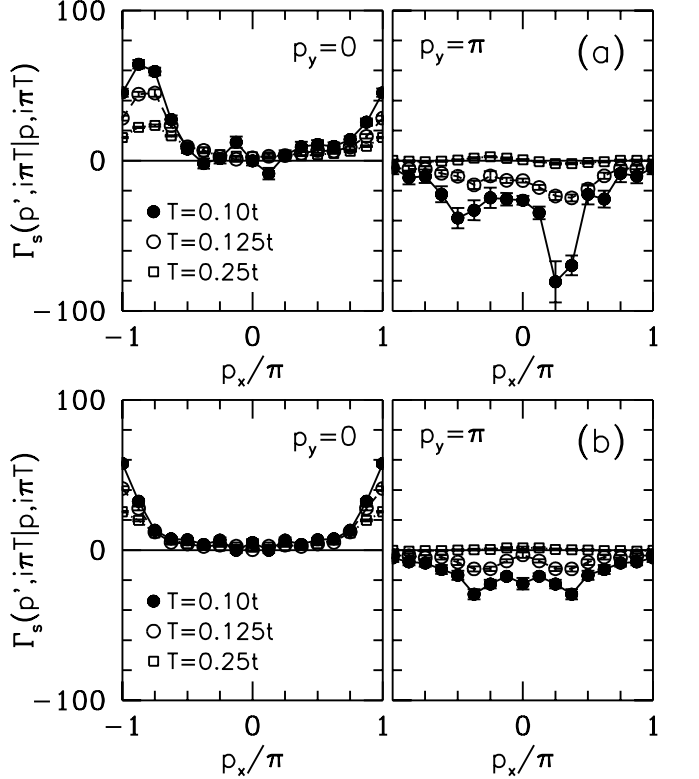


FIG. 3: Reducible particle-particle interaction in the singlet channel  $\Gamma_s(\mathbf{p}', i\pi T | \mathbf{p}, i\pi T)$  versus  $p_x$ . Here,  $p_x$  is scanned for  $p_y = 0$  (left panel) and for  $p_y = \pi$  (right panel). In (a),  $\mathbf{p}'$  is kept fixed at  $(\pi/4, \pi)$ , while in (b),  $\mathbf{p}' = (0, \pi)$ . Here,  $\Gamma_s$  is shown in units of  $t$  for  $U = 4t$ ,  $t_{\perp} = 1.6t$  and  $\langle n \rangle = 0.94$ .

crossing for the antibonding ( $p_y = \pi$ ) band occurs for  $p_x$  between  $\pi/8$  and  $\pi/4$ , while for the bonding ( $p_y = 0$ ) band there is spectral weight pinned near the Fermi level for  $3\pi/4 \leq p_x \leq \pi$  at this temperature. These results for  $A(\mathbf{p}, \omega)$  are similar to those presented in Refs. [4, 5]. In the following,  $\Gamma_s(\mathbf{p}', i\pi T | \mathbf{p}, i\pi T)$  versus  $\mathbf{p}$  will be shown for  $\mathbf{p}' = (\pi/4, \pi)$  near the Fermi level and for  $\mathbf{p}' = (0, \pi)$  at the saddle point.

Figure 3(a) shows  $\Gamma_s(\mathbf{p}', i\pi T | \mathbf{p}, i\pi T)$  versus  $\mathbf{p}$  while  $\mathbf{p}'$  is kept fixed at  $(\pi/4, \pi)$ . In the left panel,  $p_x$  is scanned from  $-\pi$  to  $\pi$  for  $p_y = 0$ , while in the right panel  $p_x$  is scanned for  $p_y = \pi$ . Here, it is seen that repulsive and attractive peaks develop in  $\Gamma_s$ , as  $T$  decreases from  $0.25t$  to  $0.1t$ . In particular, in the left panel it is seen that, when  $\mathbf{p} \approx (-3\pi/4, 0)$ , a repulsive peak develops in  $\Gamma_s$ , which corresponds to a scattering process with momentum transfer  $\mathbf{q} \approx (\pi, \pi)$  (backward scattering). In addition, in the right panel it is observed that a dip develops in  $\Gamma_s$  when  $\mathbf{p} \approx \mathbf{p}' = (\pi/4, \pi)$  corresponding to zero momentum transfer (forward scattering). This dip is due to resonant scattering in the  $d_{x^2-y^2}$ -wave BCS channel. In a three-dimensional infinite system, when a  $d_{x^2-y^2}$ -wave superconducting instability is approached,  $\Gamma_s(\mathbf{p}', i\pi T | \mathbf{p}, i\pi T)$  at the Fermi level diverges to  $+\infty$  for

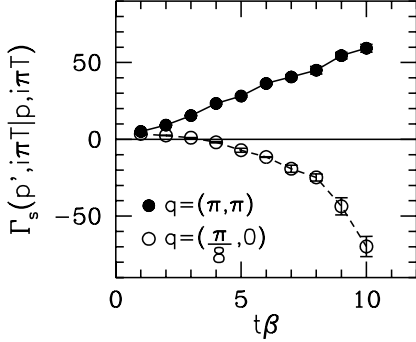


FIG. 4: Reducible particle-particle interaction in the singlet channel  $\Gamma_s(p', i\pi T | p, i\pi T)$  versus the inverse temperature  $\beta$ . Here,  $\mathbf{p} = \mathbf{p}' + \mathbf{q}$  and  $\mathbf{p}'$  is fixed at  $(\pi/4, \pi)$ . These results are for  $U = 4t$ ,  $t_\perp = 1.6t$  and  $\langle n \rangle = 0.94$ .

backward scattering, and to  $-\infty$  for forward scattering, which will be further discussed below. In Fig. 3(a), it is seen that  $\Gamma_s$  is developing this type of repulsive and attractive peaks at temperatures of order  $0.1t$ .

Figure 3(b) shows  $\Gamma_s(\mathbf{p}', i\pi T | \mathbf{p}, i\pi T)$  versus  $\mathbf{p}$  while  $\mathbf{p}'$  is kept fixed at the saddle point  $(0, \pi)$ . In this case,  $\Gamma_s$  develops a peak when  $\mathbf{p} = (\pm\pi, 0)$ , corresponding to scattering with  $\mathbf{q} = (\pi, \pi)$  momentum transfer. The magnitude of this peak is comparable to that seen in the left panel of Fig. 3(a). However, the behavior for  $\mathbf{q} = 0$  momentum transfer is different. As observed in the right panel of Fig. 3(b),  $\Gamma_s$  for  $\mathbf{q} = 0$  scattering remains pinned near zero for  $T$  down to  $0.125t$ , and becomes attractive only below this temperature. Hence, at the saddle point  $(0, \pi)$ , the resonant scattering in  $\Gamma_s$  for  $\mathbf{q} = 0$  momentum transfer is weaker compared to that at  $(\pi/4, \pi)$ .

Figure 4 shows the  $T$  dependence of the backward and forward scattering components of  $\Gamma_s$ . Here,  $\Gamma_s$  is plotted as a function of the inverse temperature  $\beta$  for momentum transfers  $\mathbf{q} = (\pi, \pi)$  and  $(\pi/8, 0)$ , while  $\mathbf{p}'$  is kept fixed at  $(\pi/4, \pi)$ . This figure shows that, near the Fermi level, the backward and forward scattering amplitudes increase rapidly at low  $T$ , becoming an order of magnitude larger than the bare Coulomb repulsion at  $T \approx 0.1t$ .

Figures 3 and 4 display the main features of  $\Gamma_s$ , which can be summarized as follows: At low  $T$ , there are strong  $\mathbf{q} \approx (\pi, \pi)$  scatterings over the whole Brillouin zone, while the  $\mathbf{q} \approx 0$  scatterings are most attractive near the Fermi surface. These features were observed at  $\langle n \rangle = 0.94$  and  $0.875$ , and for  $U = 4t$  and  $8t$ . The one-loop Renormalization-Group (RG) technique is also utilized to obtain the momentum dependence of  $\Gamma$  in the Hubbard model [8, 9]. It would be useful to make comparisons of the QMC and the RG results for the momentum dependence of  $\Gamma$  in the ladder case.

The particle-particle interaction seen in these figures is most attractive in the singlet  $d_{x^2-y^2}$ -wave pairing channel. In order to determine the strength of the pairing correlations, the Bethe-Salpeter equation for the reducible

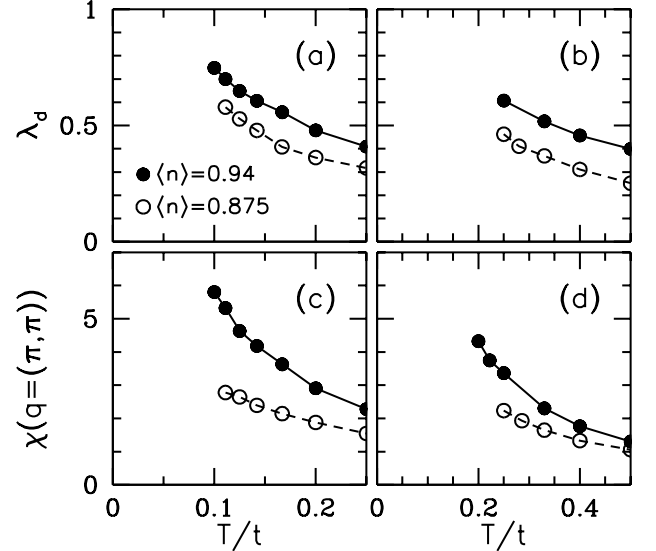


FIG. 5:  $d$ -wave irreducible eigenvalue  $\lambda_d$  of the Bethe-Salpeter equation versus  $T$  (a) for  $U = 4t$  and  $t_\perp = 1.6t$ , and (b) for  $U = 8t$  and  $t_\perp = 1.4t$ . Antiferromagnetic susceptibility  $\chi(\mathbf{q} = (\pi, \pi))$ , in units of  $t^{-1}$ , versus  $T$  (c) for  $U = 4t$  and  $t_\perp = 1.6t$ , and (d) for  $U = 8t$  and  $t_\perp = 1.4t$ . In these figures, the errorbars are smaller than the size of the symbols.

particle-particle interaction in the BCS channel,

$$\frac{\lambda_\alpha}{1 - \lambda_\alpha} \phi_\alpha(p) = -\frac{T}{N} \sum_{p'} \Gamma(p|p') |G(p')|^2 \phi_\alpha(p'), \quad (2)$$

was solved for  $\lambda_\alpha$  and the corresponding eigenfunctions  $\phi_\alpha(\mathbf{p}, i\omega_n)$ . For a three-dimensional infinite system, when the maximum  $\lambda_\alpha$  reaches 1, this signals a BCS instability to a state where the pair-wave function has the form of the corresponding eigenfunction  $\phi_\alpha(\mathbf{p}, i\omega_n)$ . For a one-dimensional system,  $\lambda_\alpha$ 's will always be less than 1, however, the  $T$  dependence of  $\lambda_\alpha$ 's gives information about the characteristic temperature scale of the pairing correlations. For instance, if the maximum eigenvalue reaches 0.9 at some temperature, then this means that the leading pairing correlations are enhanced by a factor of 10 through repeated particle-particle scatterings in the BCS channel. Hence, at this temperature, the system would exhibit strong pairing fluctuations.

At low temperatures, the maximum  $\lambda_\alpha$  of the Bethe-Salpeter equation corresponds to an eigenfunction  $\phi_d(\mathbf{p}, i\omega_n)$  which has  $d_{x^2-y^2}$  type of symmetry in the sense that it changes sign as  $\mathbf{p}$  goes from  $(\pi, 0)$  to  $(0, \pi)$  in the Brillouin zone [5]. The temperature evolution of the  $d$ -wave irreducible eigenvalue  $\lambda_d$  is shown in Figure 5(a) for  $U = 4t$  and  $t_\perp = 1.6t$ . Here, it is seen that, as  $T$  decreases,  $\lambda_d$  grows monotonically reaching 0.75 at  $T = 0.1t$  for  $\langle n \rangle = 0.94$ . Upon doping to  $\langle n \rangle = 0.875$ ,  $\lambda_d$  decreases. Also shown in Fig. 5(b) is  $\lambda_d$  for  $U = 8t$  and  $t_\perp = 1.4t$ . At the temperatures where these calculations were performed,  $\lambda_d$  is larger for  $U = 8t$ .

Next, Figures 5(c) and (d) display QMC results on the  $T$  dependence of the AFM susceptibility  $\chi(\mathbf{q} = (\pi, \pi))$  for the same parameters as in Figs. 5(a) and (b), respectively. Here  $\chi(\mathbf{q})$  is defined by

$$\chi(\mathbf{q}) = \int_0^\beta d\tau \langle m_{\mathbf{q}}^-(\tau) m_{\mathbf{q}}^+(0) \rangle \quad (3)$$

with  $m_{\mathbf{q}}^+ = \frac{1}{\sqrt{N}} \sum_{\mathbf{p}} c_{\mathbf{p}+\mathbf{q}\uparrow}^\dagger c_{\mathbf{p}\downarrow}$ ,  $m_{\mathbf{q}}^- = (m_{\mathbf{q}}^+)^*$  and  $m_{\mathbf{q}}^-(\tau) = e^{H\tau} m_{\mathbf{q}}^- e^{-H\tau}$ . Figures 5(c) and (d) show the development of the AFM correlations, as  $T$  decreases. However, as  $T \rightarrow 0$ ,  $\chi(\mathbf{q} = (\pi, \pi))$  will saturate, since the ground state of the Hubbard ladder has short-range AFM correlations. These figures also show that, upon doping at low  $T$ ,  $\lambda_d$  decays slower than  $\chi(\mathbf{q} = (\pi, \pi))$ .

During the QMC simulation, the average sign of the fermion determinants,  $\langle \text{sign} \rangle$ , determines the lowest temperatures which can be studied [10]. For  $T = 0.1t$ ,  $U = 4t$ ,  $t_\perp = 1.6t$ , and  $\langle n \rangle = 0.94$ , the value of  $\langle \text{sign} \rangle$  is 0.1. Previous calculations of  $\Gamma_s$  for the 2D [7] and the two-leg [5] Hubbard models were performed at  $T \geq 0.25t$  for  $U = 4t$  and at  $T \geq 0.5t$  for  $U = 8t$ , where  $\langle \text{sign} \rangle \approx 1.0$  and, hence, there is no sign problem.

So far in this paper,  $t_\perp \neq t$  case was considered. For isotropic hopping  $t_\perp = t$ , the Fermi-level crossings occur at  $\mathbf{p}$  near  $(\pm 3\pi/8, \pi)$  and  $(\pm 5\pi/8, 0)$ . The QMC calculations show that in this case the attractive forward scatterings in  $\Gamma_s$  are weaker, while the  $\mathbf{q} \approx (\pi, \pi)$  scatterings are as strong as for  $t_\perp = 1.6t$ . For isotropic hopping,  $\lambda_d$  is smaller than for  $t_\perp = 1.6t$ .

An important feature of the QMC data presented here is that, at sufficiently low  $T$ ,  $\Gamma_s$  near the Fermi level becomes strongly attractive for  $\mathbf{q} \approx 0$  momentum transfers for certain values of the model parameters. This is due to resonant scattering in the  $d_{x^2-y^2}$ -wave BCS channel. In order to demonstrate this effect, consider the case of an irreducible interaction  $\Gamma_I$  which is independent of frequency and separable in momentum,

$$\Gamma_I(\mathbf{p}'|\mathbf{p}) = \sum_{\alpha} V_{\alpha} g_{\alpha}(\mathbf{p}') g_{\alpha}(\mathbf{p}) \quad (4)$$

where  $\alpha$  denotes the various pairing channels. In this case, the reducible interaction is given by

$$\Gamma(\mathbf{p}'|\mathbf{p}) = \sum_{\alpha} \frac{V_{\alpha}}{1 - V_{\alpha} P_{\alpha}} g_{\alpha}(\mathbf{p}') g_{\alpha}(\mathbf{p}), \quad (5)$$

with  $P_{\alpha} = -(T/N) \sum_p g_{\alpha}^2(\mathbf{p}) |G(p)|^2$  and  $G(p)$  the single-particle Green's function. In general,  $\Gamma_I$  has both attractive and repulsive  $V_{\alpha}$ . In Eq. (5), it is seen that the repulsive components get suppressed by repeated scatterings in the BCS channel, while the attractive components get enhanced. For the  $d_{x^2-y^2}$  channel,  $g_d(\mathbf{p}) = \frac{1}{2}(\cos p_x - \cos p_y)$ . If the  $d_{x^2-y^2}$  component of  $\Gamma_I$  is attractive and gets sufficiently enhanced, here it is observed that  $\Gamma$  for  $\mathbf{q} = \mathbf{p}' - \mathbf{p} \approx 0$  can become attractive. When a

$d_{x^2-y^2}$ -wave BCS instability is approached, then, at the Fermi surface,  $\Gamma_s$  diverges to  $-\infty$  for  $\mathbf{q} \approx 0$  scatterings and to  $+\infty$  for  $\mathbf{q} \approx (\pi, \pi)$  scatterings. The important point is that, at sufficiently low  $T$ , the QMC data for  $\Gamma_s$  also exhibit this type of momentum dependence in the Hubbard ladder for certain values of the model parameters. The corresponding  $\lambda_d$  takes large values; for example,  $\lambda_d$  reaches 0.75 at  $T = 0.1t$  for  $U = 4t$  and  $\langle n \rangle = 0.94$ .

In this paper, the magnitude and the temperature scale of the  $d_{x^2-y^2}$  pairing correlations have been investigated for the two-leg Hubbard ladder. For this purpose, QMC data have been presented for the reducible particle-particle interaction  $\Gamma_s$  and the  $d_{x^2-y^2}$ -wave Bethe-Salpeter eigenvalue  $\lambda_d$ . The QMC data show that, at low  $T$ ,  $\Gamma_s$  can take values which are large compared to the bare bandwidth or the bare Coulomb repulsion. In particular, these data suggest that  $\Gamma_s$  exhibits resonant scattering in the  $d_{x^2-y^2}$  pairing channel at sufficiently low  $T$ . In addition, the dependence of the Bethe-Salpeter  $\lambda_d$  on  $U/t$ ,  $\langle n \rangle$  and  $T/t$  was discussed. These QMC data provide useful information for determining the maximum possible strength of the  $d_{x^2-y^2}$  pairing correlations in the two-leg Hubbard ladder.

The authors thank C. Honerkamp, Z.X. Shen, and T. Tohyama for helpful discussions. Part of the numerical calculations reported in this paper were carried out at the ULAKBIM High Performance Computing Center at the Turkish Scientific and Technical Research Council. One of us (N.B.) would like to thank the International Frontier Center for Advanced Materials at Tohoku University for its kind hospitality, and gratefully acknowledges support from the Japan Society for the Promotion of Science and the Turkish Academy of Sciences (EATUBA-GEBIP/2001-1-1). This work was supported by Priority-Areas Grants from the Ministry of Education, Science, Culture and Sport of Japan, NAREGI Japan and NEDO.

---

- [1] R.M. Noack, S.R. White and D.J. Scalapino, Phys. Rev. Lett. **73**, 882 (1994).
- [2] S. Gopalan, T.M. Rice and M. Sigrist, Phys. Rev. B **49**, 8901 (1994).
- [3] K. Yamaji and Y. Shimoi, Physica C **222**, 349 (1994).
- [4] R.M. Noack, N. Bulut, D.J. Scalapino and M.G. Zacher, Phys. Rev. B **56**, 7162 (1997).
- [5] T. Dahm and D.J. Scalapino, Physica C **288**, 33 (1997).
- [6] S.R. White *et al.*, Phys. Rev. B **40**, 506 (1989).
- [7] N. Bulut, D.J. Scalapino and S.R. White, Phys. Rev. B **47**, R6157 (1993); Physica C **246**, 85 (1995).
- [8] N. Furukawa, T.M. Rice and M. Salmhofer, Phys. Rev. Lett. **81**, 3195 (1998).
- [9] C. Honerkamp, M. Salmhofer, N. Furukawa and T.M. Rice, Phys. Rev. B **63**, 035109 (2001).
- [10] E.Y. Loh *et al.*, Phys. Rev. B **41**, 9301 (1990).